HHS Public Access

Author manuscript

Nucl Med Biol. Author manuscript; available in PMC 2016 May 01.

Published in final edited form as:

Nucl Med Biol. 2015 May ; 42(5): 488–493. doi:10.1016/j.nucmedbio.2014.12.008.

[^{125}I]Iodo-ASEM, a specific in vivo radioligand for α7-nAChR

Yongjun Gao[1,†], **Ronnie C. Mease**[1,†], **Thao T. Olson**[2], **Kenneth J. Kellar**[2], **Robert F. Dannals**[1], **Martin G. Pomper**[1], and **Andrew G. Horti**[1]

[1]Russell H. Morgan Department of Radiology and Radiological Science, Johns Hopkins School of Medicine, Baltimore, MD

[2]Department of Pharmacology & Physiology, Georgetown University School of Medicine, Washington, DC

Abstract

[^{125}I]Iodo-ASEM, a new radioligand with high affinity and selectivity for α7-nAChRs (K_i = 0.5 nM; α7/α4β2 = 3,414), has been synthesized in radiochemical yield of 33 ± 6% from the corresponding di-butyltriazene derivative and at high specific radioactivity (1,600 Ci/mmol; 59.2 MBq/μmol). [^{125}I]Iodo-ASEM readily entered the brains of normal CD-1 mice and specifically and selectively labeled cerebral α7-nAChRs. [^{125}I]iodo-ASEM is a new useful tool for studying α7-nAChR.

Introduction

Nicotinic cholinergic receptors (nAChRs) are neurotransmitter gated cationic channels essential to human physiology and represent an important target for drug discovery. nAChRs are found in the central nervous system (CNS), autonomic and sensory ganglia, and various non-neuronal cells. In the CNS, nAChRs mediate fast excitatory post-synaptic responses to the cognate ligand acetylcholine (ACh) and other nicotinic agonists. When nAChRs are activated with ACh, the influx of Na^+ and Ca^{2+} and efflux of K^+ are effected[1, 2].

Neuronal nAChRs are often associated with dopamine, norepinephrine, GABA, ACh and glutamate neurons, where nAChRs mediate the influence of ACh on the firing of these neurons and release of their transmitters [3]. Neuronal nAChRs are composed of various α and β subunits that can assemble into pentamers[4] with α4β2-nAChR and α7-nAChR subtypes together representing the highest concentration of nAChRs in the CNS[5]. The functional properties of different subtypes of nAChRs reflect their respective roles in regulating physiology, which are diverse and include memory, sensory gating, metabolism and inflammation. The α7-nAChR is involved in pathogenesis of a variety of psychiatric

†Contributed equally

and neurological disorders including schizophrenia (SCZ) and Alzheimer's disease (AD), as well as disorders in the periphery such as cancer and macrophage chemotaxis [1, 4, 6–9].

Recent studies indicate that the α7-nAChR is an important target for drug development in SCZ, and selective partial agonists of the α7-nAChR improve cognitive performance in these patients [10, 11]. Several emerging drugs that are selective for α7-nAChRs are currently in clinical phases of development for treatment of various disorders, including SCZ [4, 11–13]. A number of post-mortem studies have demonstrated a reduction of α7-nAChR binding and expression in the brain tissue of subjects with SCZ [11].

A characteristic of AD is degeneration of cholinergic neurons and reduction of nAChR expression [14]. A number of reports have described a significant reduction in α7-nAChRs in the cortex and hippocampus of patients with AD [14–17], although several studies were unable to confirm these results [11, 18, 19]. The inconsistency of these results may be due to variability of α7-nAChRs in AD brain at different stages of the disease [11, 20]. AD is associated with cognitive impairment and modulators of the α7-nAChR have been studied extensively for the treatment of cognitive deficits in AD [21, 22].

Other studies have demonstrated a role for α7-nAChRs in the neural cholinergic-anti-inflammatory pathway via the vagus nerve because activation of this receptor prevents release of cytokines [23]. The activity of α7-nAChRs on macrophages and other cytokine-secreting cells is a rapidly expanding field of study [24–26].

Despite intense research the role of α7-nAChRs in the brain is not fully understood. Positron emission tomography (PET) and single-photon emission computed tomography (SPECT) are the most advanced techniques to map and quantify cerebral receptors and their occupancy by neurotransmitters and drugs in human subjects. Recently we developed the first highly specific radioligand, [^{18}F]ASEM, for PET imaging of α7-nAChR in animals[27, 28] and human subjects[29]. Here we present [^{125}I]iodo-ASEM, a radioiodinated analog of [^{18}F]ASEM designed for use in cell-based assays and pre-clinical in vivo studies. In addition, the [^{125}I]iodo-ASEM is amenable to radiolabeling with ^{123}I and use as a radiotracer for human SPECT.

Materials and Methods

General

All reagents were used directly as obtained commercially unless otherwise noted. All moisture-sensitive reactions were performed under an argon atmosphere using oven-dried glassware and anhydrous solvents. Column flash chromatography was carried out using E. Merck silica gel 60F (230–400 mesh). Analytical thin-layer chromatography (TLC) was performed on aluminum sheets coated with silica gel 60 F_{254} (0.25 mm thickness, E. Merck, Darmstadt, Germany).

^{1}H NMR spectra were recorded with a Bruker-400 NMR spectrometer at nominal resonance frequencies of 400 MHz, in $CDCl_3$ or DMSO-d_6 (referenced to internal Me_4Si at δ_H 0 ppm). The chemical shifts (δ) were expressed in parts per million (ppm). First order *J* values were

given in Hertz. Splitting patterns are described as singlet (s), doublet (d), triplet (t), quartet (q), and broad (br).

The radio-high performance liquid chromatography (HPLC) system consisted of two Varian ProStar pumps, a single Rheodyne Model 7725i manual injector, a ProStar 325 UV-Vis variable wavelength detector, and an in-line BioScan Flow-Count radioactivity detector. All HPLC chromatograms were recorded with Varian Galaxy software (version 1.8). Analytical and semi-preparative chromatography was performed using Phenomenex Luna C-18 10 μm columns (analytical 4.6 × 250 mm and semi-preparative 10 × 250 mm).

Chemistry

3-(1,4-Diazabicyclo[3.2.2]nonan-4-yl)-6-[3,3-(1,4-butanediyl)triazeno]dibenzo[b,d]thiophene 5,5-dioxide (2)—6-Amino-3-(1,4-diazabicyclo[3.2.2]nonan-4-yl)dibenzo[b,d]thiophene 5,5-dioxide[27] **1** (172 mg, 0.38 mmol) was dissolved in CH_3CN (0.4 mL) at room temperature, and then concentrated HCl (0.16 mL, 5.0 eq.) was added. The mixture was cooled to −5 °C. A solution of $NaNO_2$ (31 mg, 0.46 mmol, in 0.4 mL cold water) was added dropwise. The resulting solution of the diazonium salt was stirred for 30 min and then added to a solution of pyrrolidine (32 mg, 1.2 eq.) and K_2CO_3 (0.95 mmol, 2.5 eq.) in CH_3CN/water (1.2 mL, 1:1), which was previously cooled to −5 °C. The reaction mixture was warmed to room temperature and stirred for 1h. The mixture was evaporated and dried. The solid was purified by chromatography (20 g silica gel, 10:1:0.1 $CHCl_3$:*i*-PrOH:Et_3N). The fractions containing the product were combined and evaporated, then washed with water and dried to give compound **2** (86 mg, 52%). ^{1}H NMR (DMSO-d_6, 400 MHz) δ 7.80 (d, *J*=8.0 Hz, 1H), 7.57-7.52 (m, 2H), 7.30 (d, *J*=8.0 Hz, 1H), 7.08-7.04 (m, 2H), 4.15 (s, 1H), 3.99-3.96 (m, 2H), 3.68-3.63 (m, 6H), 2.06-1.99 (m, 6H), 1.71-1.66 (m, 2H).

3-(1,4-Diazabicyclo[3.2.2]nonan-4-yl)-6-(3,3-dibutyltriazeno)dibenzo[b,d]thiophene 5,5-dioxide (3)

Method 1: 6-Amino-3-(1,4-diazabicyclo[3.2.2]nonan-4-yl)dibenzo[b,d]thiophene 5,5-dioxide[27] (**1**) (118 mg, 0.33 mmol) was dissolved in CH_3CN (0.8 mL) at room temperature, and then concentrated HCl (0.133 mL, 5.0 eq.) was added. The mixture was cooled to −5 °C. A solution of $NaNO_2$ (30 mg, 0.43 mmol, in 0.3 mL cold water) was added dropwise. The resulted solution of the intermediate diazonium salt was stirred for 40 min and then added to a solution of dibutylamine (65 mg, 1.5 eq.) and K_2CO_3 (228 mg, 1.65 mmol, 5 eq.) in CH_3CN/water (1 mL, 1:1), which was previously cooled to −5 °C. The reaction mixture was warmed to room temperature and stirred for 1h. The mixture was evaporated and dried. The solid was purified by chromatography (100 g silica gel, 1–10% gradient of $CHCl_3$:*i*-PrOH:Et_3N). The fractions containing the product were combined and evaporated and washed with water, dried to yield compound **3** (66 mg, 40%).

Method 2: A catalyst solution was prepared by mixing tris(dibenzylideneacetone)dipalladium ($Pd_2(dba)_3$; 33 mg, 0.037 mmol; 5% eq.) and racemic 2,2′-bis(diphenylphosphino)-1,1′-binaphthyl (BINAP; 47 mg, 0.075 mmol, 10% equivalents) in toluene (5 mL) and heating the mixture at 85°C. for 15 min. The solution

was cooled, and then added to a mixture of 1,4-diazabicyclo[3.2.2]nonane (133 mg, 1.09 mmol) and 3-bromo-6-(3,3-dibutyltriazeno)dibenzo[*b*,*d*]thiophene 5,5-dioxide (**6**) (350 mg, 0.78 mmol), in toluene (15 mL). Cs_2CO_3 (252 mg, 0.78 mmol) was then added, and the reaction mixture was flushed with nitrogen and heated to 85°C for 28 h. (HPLC showed the reaction was complete.) After cooling to room temperature, the mixture was concentrated and purified by chromatography on silica gel ($CHCl_3$:*i*-PrOH:Et_3N 10:1:0.1). The desired fractions containing product were combined and evaporated to remove solvents. The resulted yellow solid was washed with water and dried to yield compound **3** (387 mg, 88% yield); ^{1}H NMR (DMSO-d_6, 400 MHz) δ 7.81 (d, *J*=8.0 Hz, 1H), 7.57-7.51 (m, 2H), 7.32 (d, *J*=8.0 Hz, 1H), 7.15 (br s, 1H), 7.07 (d, *J*=8.0 Hz, 2H), 4.18 (s, 1H), 3.84-3.66 (m, 6H), 3.68-3.63 (m, 6H), 2.99-2.89 (m, 6H), 2.07-2.01 (m, 2H), 1.74-1.68 (m, 6H), 1.37-1.31 (m, 4H), 0.94 (s, 3H), 0.93 (s, 3H).

6-Amino-3-bromodibenzo[b,d]thiophene 5,5-dioxide (5)—A mixture of 3-bromo-6-nitrodibenzo[b,d]thiophene 5,5-dioxide (**4**)[27] (1.525 g, 4.47 mmol), iron powder (1.03 g, 14.6 mmol), and ammonium chloride (305 mg, 5.59 mmol) in a tetrahydrofuran (THF) (30 mL), methanol (30 mL), and water (10 mL) was heated to reflux (80 °C) for 3 h. The resulting mixture was diluted with ethanol and concentrated and dried under vacuum. The residue was purified by silica gel column chromatography ($CHCl_3$:*i*-PrOH 50:1) to give compound **5** (1.26 g, 91%). ^{1}H NMR (DMSO-d_6, 400 MHz) δ 8.42 (s, 1H), 8.20 (d, *J*=8.0 Hz, 1H), 8.10-8.06 (m, 2H), 7.92-7.87 (m, 1H), 7.58 (t, *J*=8.0 Hz, 1H).

3-Bromo-6-(3,3-dibutyltriazeno)dibenzo[b,d]thiophene 5,5-dioxide (6)—Concentrated HCl (0.6 mL, 5.0 eq.) was added to a mixture of 6-amino-3-bromodibenzo[b,d]thiophene 5,5-dioxide (**5**) (465 mg, 1.5 mmol) in CH_3CN (4 mL) at room temperature and the resulting solution was chilled to −5 °C. A solution of $NaNO_2$ (135 mg, 1.93 mmol) in 0.9 mL cold water was added dropwise. The resulting solution of the diazonium salt was stirred for 40 min and then added to a solution of dibutylamine (293 mg, 1.5 eq.) and K_2CO_3 (1027 mg, 2.48 mmol, 5 eq) in CH_3CN/water (3 mL, 1:1), which was previously cooled to −5 °C. The reaction mixture was warmed to room temperature and stirred for 1h. The mixture was evaporated and dried. The solid was purified by chromatography (100 g silica gel, gradient of $CHCl_3$:*i*-PrOH). The fractions containing the product were combined and evaporated, then washed with water, and dried to afford compound **6** (391 mg, 58%). ^{1}H NMR ($CDCl_3$, 400 MHz) δ 7.94 (s, 1H), 7.72 (d, *J*=8.0 Hz, 1H), 7.64-7.59 (m, 2H), 7.62 (t, *J*=8.0 Hz, 1H), 7.42 (d, *J*=8.0 Hz, 1H), 3.88-3.82 (m, 4H), 1.79-1.75 (m, 4H), 1.48-1.40 (m, 4H), 1.01 (s, 3H), 1.00 (s, 3H).

Radiochemistry

3-(1,4-Diazabicyclo[3.2.2]nonan-4-yl)-6-[^{125}I]iododibenzo[b,d]thiophene 5,5-dioxide ([^{125}I]iodo-ASEM)—To a solution of triazene **3** (1 mg, 0.002 mmol) in CH_3CN (0.1 mL) was added 7 mCi of $Na^{125}I$ in 0.1 N NaOH at room temperature, followed by water (10 μL) and TFA (10 μL, 67.5 eq.). The mixture was heated at 80 °C in a sand bath for 20 min. The reaction mixture was cooled, diluted with a CH_3CN/water mixture (1/1, 50 μL) and applied to a reverse phase semi-preparative HPLC column (Phenomenex Luna C18 250 × 10 mm, 10 micron; mobile phase: 28/72/0.1 acetonitrile/water/TFA; flow rate 6 mL/min).

[^{125}I]iodo-ASEM elutes at 20.5 min. The radioactive peak was collected, diluted with water (50 mL) and loaded onto an activated (sequential ethanol and water washes) Waters C-18 Oasis HLB Light solid-phase extraction (SPE) cartridge. After the SPE was washed with 10 mL of saline, the product was eluted with a mixture of 1 mL of ethanol and 0.04 mL of 1 N HCl into a multidose vial and 10 mL of 0.9% saline and 0.05 mL of sterile 8.4% solution sodium bicarbonate were added to the vial through the same SPE cartridge. The final product [^{125}I]iodo-ASEM was then analyzed by HPLC using a UV detector at 340 nm to determine the radiochemical purity and specific radioactivity at the time the synthesis ended. The total synthesis time including QC was 70–80 min. Radiochemical yield: 33 ± 6% (n=4); specific activity: 1,600 Ci/mmol (59.2 GBq/mmol).

In vitro inhibition binding affinity studies

Inhibition binding affinity constants (K_i) of iodo-ASEM were determined in membranes from HEK293 cells that heterologously express α7, α3β4 and α4β2 nAChRs, as described previously[3, 30].

[^{125}I]iodo-ASEM biodistribution studies in CD-1 mice

Baseline study: Male, CD-1 mice weighing 25–30 g from Charles River Laboratories, (Wilmington, MA) were used for biodistribution studies. The animals were sacrificed by cervical dislocation at various times (three animals per time point) following injection of [^{125}I]iodo-ASEM (3 μCi, specific radioactivity 1600 mCi/μmol, in 0.2 mL saline) into a lateral tail vein. The brains were removed and dissected on ice. The brain regions of interest were weighed and their radioactivity content was determined in an automated γ-counter. Aliquots of the injectate were prepared as standards and their radioactivity content was counted along with the tissue samples. The percent of injected dose per gram of tissue (%ID/g tissue) was calculated. All experimental protocols were approved by the Animal Care and Use Committee of the Johns Hopkins Medical Institutions.

Blockade of [^{125}I]iodo-ASEM binding: *In vivo* CB1 receptor blocking studies were carried out by subcutaneous (s.c.) administration of various blockers (SSR180,711 – 2 mg/kg; ondansetron – 2 mg/kg; cytisine – 0.5 mg/kg) followed by i.v. injection of [^{125}I]iodo-ASEM (3 μCi, specific radioactivity ~1600 mCi/μmol, 0.2 mL) 5 min thereafter. The blocker dosage is based on the previous blocking studies with α7-nAChR PET tracer [^{18}F]ASEM [27, 28] and α4β2-nAChR tracer [^{18}F]AZAN [31, 32]. The drugs were dissolved in saline and administered in a volume of 0.1 mL. Control animals were injected with 0.1 mL of saline. Three hours after administration of the tracer, brain tissues were harvested, and their radioactivity content was determined.

Results and Discussion

Chemistry

Synthesis of triazene precursors for [^{125}I]iodo-ASEM—Two triazene precursors **2** and **3** for radioiodination of [^{125}I]iodo-ASEM have been synthesized by diazotization of amino derivative **1**[27] in the presence of pyrrolidine or dibutylamine, respectively (Scheme 1).

The model iodination reaction was performed by acidic conversion of **2** or **3** to the diazonium intermediate and further reaction obtained with sodium iodide in the solution of aqueous acetonitrile. In the model iodination reaction, the conversion of both precursors **2** and **3** to unlabeled iodo-ASEM (Scheme 2) was observed. However, a suitable preparative reverse-phase HPLC separation of iodo-ASEM was only achieved with the more hydrophobic precursor **3.** The separation of iodo-ASEM and **2** was very challenging owing to the similar retention time of both compounds.

After achieving a good yield of iodo-ASEM in the model iodination reaction with precursor **3**, a more practical and economical reaction route for scale up of the synthesis of this precursor was explored. The improved synthesis of **3** (Scheme 1) started with nitro-compound **4** that was smoothly reduced by iron powder in ammonium chloride solution to give amine **5** in 91% yield. Diazotization of amine **5** using sodium nitrite in hydrochloric acid solution followed by diazo coupling with an excess of dibutyamine in the presence of potassium carbonate gave the triazene compound **6** in 58% yield. The Buchwald-Hartwig cross-coupling reaction between compound **6** and 1,4-diazabicyclo[3.2.2]nonane afforded **3** in 88% yield.

Radiochemistry—[^{125}I]Iodo-ASEM was prepared by the reaction of the triazene **3** with no-carrier added Na^{125}I in the presence of trifluoroacetic acid in a solution of aqueous acetonitrile as solvent. The final product was purified by semi-preparative reverse-phase HPLC followed by solid-phase extraction. The final product was obtained with a radiochemical yield of 33 ± 6% (n=4) at the end-of-synthesis (non-decay-corrected), and a specific radioactivity of 1,600 Ci/mmol (59.2 MBq/μmol), and radiochemical purity greater than 98%.

In vitro inhibition binding assay of iodo-ASEM—In our previous studies we demonstrated high α7-nAChR binding affinity of iodo-ASEM (K_i = 0.93 and 1.93 nM) in competition for [^{125}I]α-bungarotoxin binding sites in rat cortical membranes. Here, the inhibition binding constants of iodo-ASEM at α7-, α3β4- and α4β2-nAChR subtypes expressed in HEK-293 cells were determined in competition with [^{3}H]epibatidine as the radiotracer (Table 1) using the general method described previously[3, 30]. The sub-nanomolar α7 binding affinity (0.5 nM) and high selectivity (3,414) versus the other major cerebral nicotinic subtype α4β2-nAChR suggests that radiolabeled [^{125}I]iodo-ASEM will be very useful as a tool for studying α7-nAChR in vitro and in vivo.

Regional brain distribution studies in CD-1 mice

Baseline study: [^{125}I]Iodo-ASEM was evaluated in CD-1 mice to determine regional distribution within brain after intravenous injection. [^{125}I]Iodo-ASEM exhibited high regional brain uptake, which correlated with target areas known to contain relatively high concentrations of α7-nAChR, with peak uptake (5.2 percentage injected dose per gram of tissue, %ID/g) at 20 min post-injection followed by decline. The highest accumulation of radioactivity occurred in the superior/inferior colliculus, hippocampus and cortex. Moderate uptake was observed in the rest of brain and the lowest radioactivity was seen in cerebellum (Table 2). This distribution of radioactivity was similar to the previously published

autoradiography data on the distribution of α7-nAChRs in rodents[33, 34] and in vivo distribution of [^{18}F]ASEM in mice[27, 28]. The clearance rate of [^{125}I]iodo-ASEM from cerebellum was higher than that from any other region. The colliculus to cerebellum ratios reached a maximum of 4.2 at 180 min post-injection. A previously studied radioiodinated α7-nAChR radioligand (*1S,2R,4S*)-5′-(2-[^{125}I]iodofuran-3-yl)-3′H-4-azaspiro[bicyclo[2.2.2]octane-2,2′-furo[2,3-b]pyridine] exhibited a lower ratio (~2.5)[35].

a7-nAChR binding specificity: A blocking dose of the α7-nAChR selective partial agonist SSR180711[36] significantly inhibited [^{125}I]iodo-ASEM binding in the α7-nAChR-rich superior and inferior colliculi and hippocampus at 180 min post-injection, but the blockade was negligible in the α7-nAChR - poor cerebellum (Fig. 1). This blocking demonstrated that [^{125}I]iodo-ASEM uptake in the α7-nAChR - rich regions is specific and mediated by α7-nAChR.

a7-nAChR binding selectivity versus α4β2-nAChR and 5-HT$_3$: For determination of *in vivo* α7-nAChR selectivity of [^{125}I]iodo-ASEM versus other receptors, we compared in a separate experiment the regional distribution (Fig. 2) of the radiotracer in control CD-1 mice and mice pre-injected with cytisine or ondansetron. Cytisine is a partial nicotinic agonist selective for α4β2-nAChR and other β2-containing heteromeric nAChR subtypes with very low α7-nAChR binding affinity[3, 30, 37] and ondansetron is a selective 5-HT$_3$ antagonist[38]. Most previous α7-nAChR PET and SPECT radiotracers suffered a lack of selectivity versus 5-HT$_3$ and/or the second major nicotinic receptor subtype α4β2-nAChR[39]. In this study, neither cytisine nor ondansetron reduced the accumulation of [^{125}I]iodo-ASEM radioactivity in the mouse brain when compared with mice injected with vehicle (Fig. 2). This demonstrates that in the mouse brain the [^{125}I]iodo-ASEM binding is selective for α7-nAChRs versus 5-HT$_3$ and α4β2-nAChR which is in agreement with the high α7-nAChR selectivity of the structurally similar PET radioligand [^{18}F]ASEM that was observed previously[27, 28].

Conclusion

[^{125}I]Iodo-ASEM, a high affinity and selective α7-nAChR radioligand, was prepared by radioiodination of the corresponding di-butyltriazene derivative. [^{125}I]iodo-ASEM readily enters the mouse brain, specifically and selectively labels α7-nAChRs and has a substantially greater value for the region-to-cerebellum ratio than the previously reported radioiodinated radiotracers. [^{125}I]iodo-ASEM is a valuable small molecule tool for studying α7-nAChR in vivo and in vitro. SPECT studies with [^{123}I]iodo-ASEM are in progress.

Acknowledgments

We thank Ms. Paige Finley for help with animal experiments and Judy W. Buchanan for editorial help. This research was supported by NIH grant AG037298 (AGH) and, in part, by Division of Nuclear Medicine of The Johns Hopkins University School of Medicine.

References

1. Albuquerque EX, Pereira EF, Alkondon M, Rogers SW. Mammalian nicotinic acetylcholine receptors: from structure to function. Physiol Rev. 2009; 89:73–120. [PubMed: 19126755]

2. Kellar, KJ.; Xiao, Y. Neuronal nicotinic receptors: one hundred years of progress. In: Sibley, DR., editor. Handbook of contemporary neuropharmacology. Wiley-Interscience; 2007. p. 108-31.
3. Xiao Y, Kellar K. The comparative pharmacology and up-regulation of rat neuronal nicotinic receptor subtype binding sites stably expressed in transfected mammalian cells. J Pharmacol Exp Ther. 2004; 310:98–107. [PubMed: 15016836]
4. D'Hoedt D, Bertrand D. Nicotinic acetylcholine receptors: an overview on drug discovery. Expert Opin Ther Targets. 2009; 13:395–411. [PubMed: 19335063]
5. Lukas RJ, Changeux JP, Le Novere N, Albuquerque EX, Balfour DJ, Berg DK, et al. International Union of Pharmacology. XX. Current status of the nomenclature for nicotinic acetylcholine receptors and their subunits. Pharmacol Rev. 1999; 51:397–401. [PubMed: 10353988]
6. Ishikawa M, Hashimoto K. alpha7 nicotinic acetylcholine receptor as a potential therapeutic target for schizophrenia. Curr Pharm Des. 2011; 17:121–9. [PubMed: 21355839]
7. Parri HR, Hernandez CM, Dineley KT. Research update: Alpha7 nicotinic acetylcholine receptor mechanisms in Alzheimer's disease. Biochem Pharmacol. 2011; 82:931–42. [PubMed: 21763291]
8. Woodruff-Pak DS, Gould TJ. Neuronal nicotinic acetylcholine receptors: involvement in Alzheimer's disease and schizophrenia. Behav Cogn Neurosci Rev. 2002; 1:5–20. [PubMed: 17715584]
9. Hoffmeister PG, Donat CK, Schuhmann MU, Voigt C, Walter B, Nieber K, et al. Traumatic brain injury elicits similar alterations in alpha7 nicotinic receptor density in two different experimental models. Neuromolecular Med. 2011; 13:44–53. [PubMed: 20857232]
10. Olincy A, Harris JG, Johnson LL, Pender V, Kongs S, Allensworth D, et al. Proof-of-concept trial of an alpha7 nicotinic agonist in schizophrenia. Arch Gen Psychiatry. 2006; 63:630–8. [PubMed: 16754836]
11. Thomsen MS, Hansen HH, Timmerman DB, Mikkelsen JD. Cognitive improvement by activation of alpha7 nicotinic acetylcholine receptors: from animal models to human pathophysiology. Curr Pharm Des. 2010; 16:323–43. [PubMed: 20109142]
12. Taly A, Charon S. alpha7 nicotinic acetylcholine receptors: a therapeutic target in the structure era. Curr Drug Targets. 2012; 13:695–706. [PubMed: 22300037]
13. Wallace TL, Bertrand D. Alpha7 neuronal nicotinic receptors as a drug target in schizophrenia. Expert Opin Ther Targets. 2013; 17:139–55. [PubMed: 23231385]
14. Auld DS, Kornecook TJ, Bastianetto S, Quirion R. Alzheimer's disease and the basal forebrain cholinergic system: relations to beta-amyloid peptides, cognition, and treatment strategies. Prog Neurobiol. 2002; 68:209–45. [PubMed: 12450488]
15. Davies P, Feisullin S. Postmortem stability of alpha-bungarotoxin binding sites in mouse and human brain. Brain Res. 1981; 216:449–54. [PubMed: 7248786]
16. Aubert I, Araujo DM, Cecyre D, Robitaille Y, Gauthier S, Quirion R. Comparative alterations of nicotinic and muscarinic binding sites in Alzheimer's and Parkinson's diseases. J Neurochem. 1992; 58:529–41. [PubMed: 1729398]
17. Sugaya K, Giacobini E, Chiappinelli VA. Nicotinic acetylcholine receptor subtypes in human frontal cortex: Changes in Alzheimer's disease. J Neurosci Res. 1990; 27:349. [PubMed: 2097379]
18. Hellstrom-Lindahl E, Mousavi M, Zhang X, Ravid R, Nordberg A. Regional distribution of nicotinic receptor subunit mRNAs in human brain: comparison between Alzheimer and normal brain. Brain Res Mol Brain Res. 1999; 66:94–103. [PubMed: 10095081]
19. Lang W, Henke H. Cholinergic receptor binding and autoradiography in brains of non-neurological and senile dementia of Alzheimer-type patients. Brain Res. 1983; 267:271–80. [PubMed: 6871676]
20. Court J, Martin-Ruiz C, Piggott M, Spurden D, Griffiths M, Perry E. Nicotinic receptor abnormalities in Alzheimer's disease. Biol Psychiatry. 2001; 49:175–84. [PubMed: 11230868]
21. Lippiello PM, Bencherif M, Hauser TA, Jordan KG, Letchworth SR, Mazurov AA. Nicotinic receptors as targets for therapeutic discovery. Expert Opinion on Drug Discovery. 2007; 2:1185–203. [PubMed: 23496128]
22. Kem WR. The brain alpha7 nicotinic receptor may be an important therapeutic target for the treatment of Alzheimer's disease: studies with DMXBA (GTS-21). Behav Brain Res. 2000; 113:169–81. [PubMed: 10942043]

23. Borovikova LV, Ivanova S, Zhang M, Yang H, Botchkina GI, Watkins LR, et al. Vagus nerve stimulation attenuates the systemic inflammatory response to endotoxin. Nature. 2000; 405:458–62. [PubMed: 10839541]
24. Gallowitsch-Puerta M, Tracey KJ. Immunologic role of the cholinergic anti-inflammatory pathway and the nicotinic acetylcholine alpha 7 receptor. Ann N Y Acad Sci. 2005; 1062:209–19. [PubMed: 16461803]
25. Bencherif M, Lippiello PM, Lucas R, Marrero MB. Alpha7 nicotinic receptors as novel therapeutic targets for inflammation-based diseases. Cell Mol Life Sci. 2011; 68:931–49. [PubMed: 20953658]
26. Marrero MB, Bencherif M, Lippiello PM, Lucas R. Application of alpha7 nicotinic acetylcholine receptor agonists in inflammatory diseases: an overview. Pharm Res. 2011; 28:413–6. [PubMed: 20859658]
27. Gao Y, Kellar KJ, Yasuda RP, Tran T, Xiao Y, Dannals RF, et al. Derivatives of Dibenzothiophene for Positron Emission Tomography Imaging of alpha7-Nicotinic Acetylcholine Receptors. J Med Chem. 2013; 56:7574–89. [PubMed: 24050653]
28. Horti AG, Gao Y, Kuwabara H, Wang Y, Abazyan S, Yasuda RP, et al. 18F-ASEM, a Radiolabeled Antagonist for Imaging the alpha7-Nicotinic Acetylcholine Receptor with PET. J Nucl Med. 2014; 55:672–7. [PubMed: 24556591]
29. Wong DF, Kuwabara H, Pomper M, Holt DP, Brasic JR, George N, et al. Human Brain Imaging of alpha7 nAChR with [(18)F]ASEM: a New PET Radiotracer for Neuropsychiatry and Determination of Drug Occupancy. Mol Imaging Biol. 2014; 16:730–8. [PubMed: 25145965]
30. Xiao Y, Abdrakhmanova GR, Baydyuk M, Hernandez S, Kellar KJ. Rat neuronal nicotinic acetylcholine receptors containing alpha7 subunit: pharmacological properties of ligand binding and function. Acta Pharmacol Sin. 2009; 30:842–50. [PubMed: 19448648]
31. Gao Y, Kuwabara H, Spivak CE, Xiao Y, Kellar K, Ravert HT, et al. Discovery of (-)-7-Methyl-2-exo-[3′-(6-[18F]fluoropyridin-2-yl)-5′-pyridinyl]-7-azabicyclo[2.1]heptane, a Radiolabeled Antagonist for Cerebral Nicotinic Acetylcholine Receptor (α4β2-nAChR) with Optimal Positron Emission Tomography Imaging Properties. J Med Chem. 2008; 51:4751–64. [PubMed: 18605717]
32. Kuwabara H, Wong DF, Gao Y, Valentine H, Holt DP, Ravert HT, et al. PET Imaging of nicotinic acetylcholine receptors in baboons with 18F-AZAN, a radioligand with improved brain kinetics. J Nucl Med. 2012; 53:121–9. [PubMed: 22173841]
33. Clarke PB, Schwartz RD, Paul SM, Pert CB, Pert A. Nicotinic binding in rat brain: autoradiographic comparison of [3H]acetylcholine, [3H]nicotine, and [125I]-alpha-bungarotoxin. J Neurosci. 1985; 5:1307–15. [PubMed: 3998824]
34. Whiteaker P, Davies AR, Marks MJ, Blagbrough IS, Potter BV, Wolstenholme AJ, et al. An autoradiographic study of the distribution of binding sites for the novel alpha7-selective nicotinic radioligand [3H]-methyllycaconitine in the mouse brain. Eur J Neurosci. 1999; 11:2689–96. [PubMed: 10457165]
35. Pomper MG, Phillips E, Fan H, McCarthy DJ, Keith RA, Gordon JC, et al. Synthesis and biodistribution of radiolabeled alpha 7 nicotinic acetylcholine receptor ligands. J Nucl Med. 2005; 46:326–34. [PubMed: 15695794]
36. Biton B, Bergis OE, Galli F, Nedelec A, Lochead AW, Jegham S, et al. SSR180711, a novel selective alpha7 nicotinic receptor partial agonist: (1) binding and functional profile. Neuropsychopharmacology. 2007; 32:1–16. [PubMed: 17019409]
37. Rollema H, Shrikhande A, Ward KM, Tingley FD 3rd, Coe JW, O'Neill BT, et al. Pre-clinical properties of the alpha4beta2 nicotinic acetylcholine receptor partial agonists varenicline, cytisine and dianicline translate to clinical efficacy for nicotine dependence. Br J Pharmacol. 2010; 160:334–45. [PubMed: 20331614]
38. Ye JH, Ponnudurai R, Schaefer R. Ondansetron: a selective 5-HT(3) receptor antagonist and its applications in CNS-related disorders. CNS Drug Rev. 2001; 7:199–213. [PubMed: 11474424]
39. Ravert HT, Dorff P, Foss CA, Mease RC, Fan H, Holmquist CR, et al. Radiochemical synthesis and in vivo evaluation of [18F]AZ11637326: An agonist probe for the alpha7 nicotinic acetylcholine receptor. Nucl Med Biol. 2013; 40:731–9. [PubMed: 23680470]

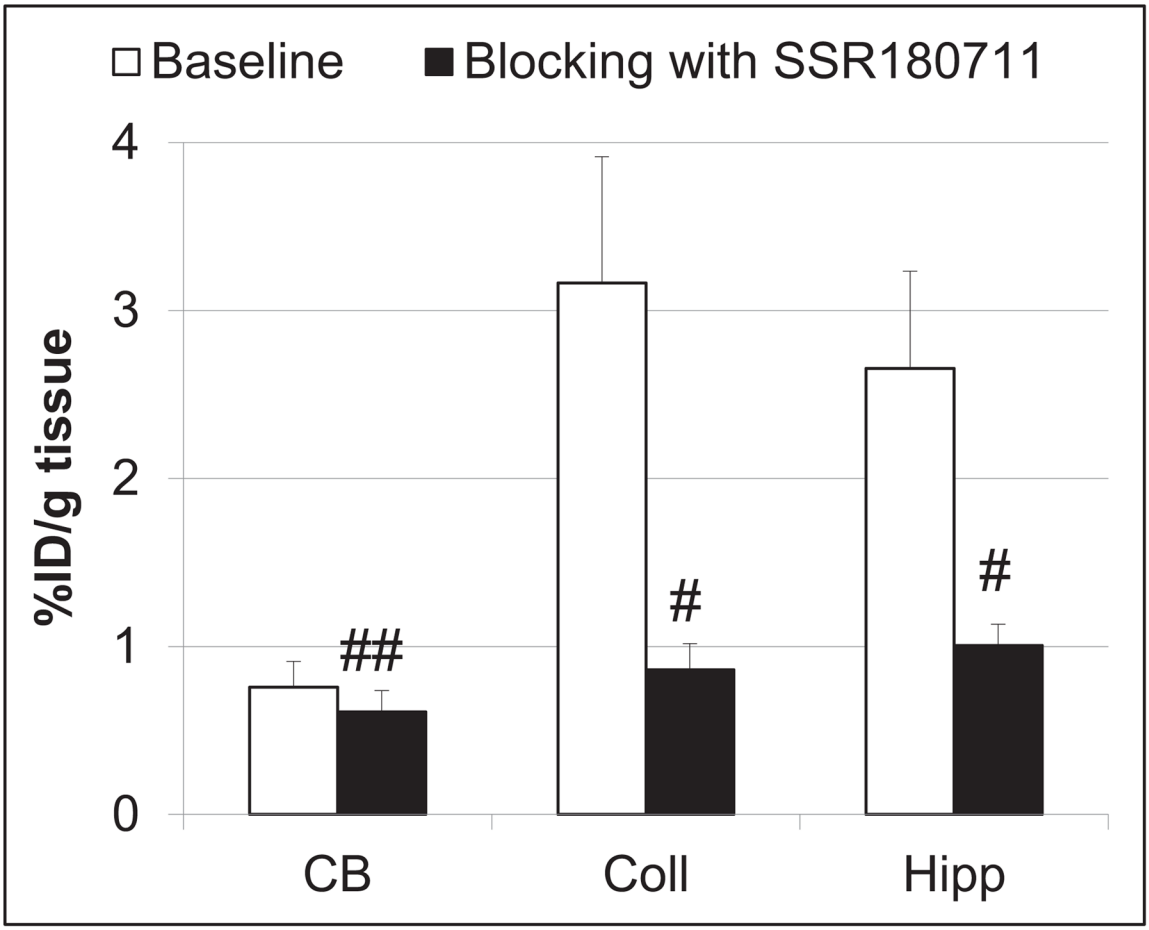

Figure 1.

Comparison of regional brain uptake of [^{125}I]iodo-ASEM in mice at 180 min post-injection in control (white bars) and after blocking with SSR180711 (2 mg/kg, s.c.) (black bars). There was significant blocking in all regions except cerebellum. CB = cerebellum; Coll = superior & inferior colliculi; Hipp = hippocampus. Data are mean ± SD (n = 3). $^{\#}P < 0.01$, significantly different from controls; $^{\#\#}P = 0.27$, not significantly different from controls (ANOVA)

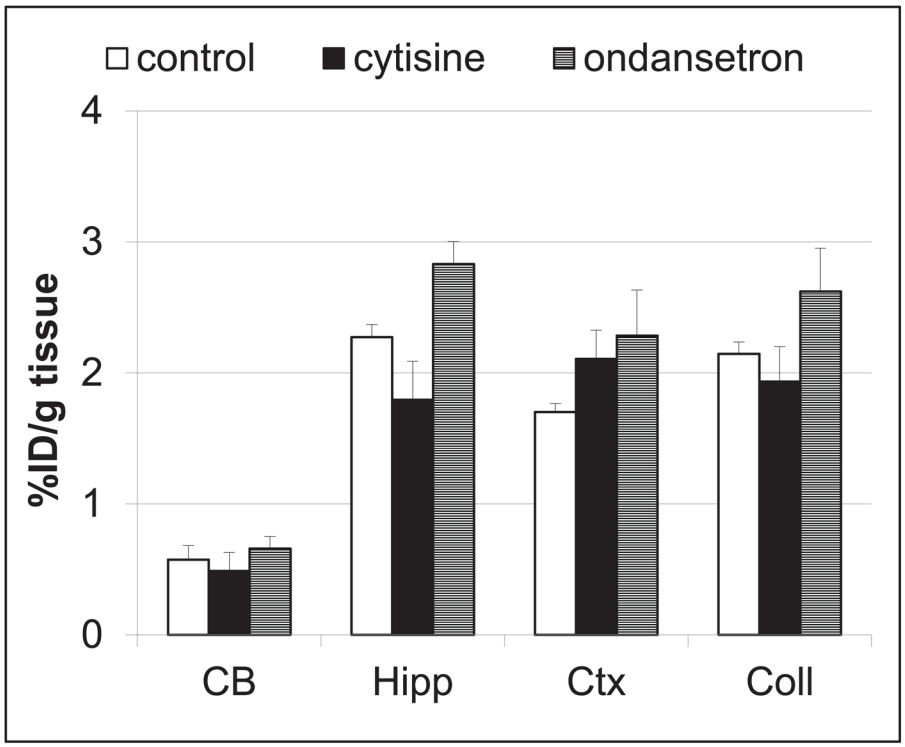

Figure 2.

Blockade of [^{125}I]iodo-ASEM accumulation in CD-1 mouse brain regions by injection of ondansetron (2 mg/kg, s.c.) and cytisine (0.5 mg/kg, s.c.) at 180 min time-point after the radiotracer injection. Data: mean %injected dose/g tissue ± SD (n = 3). Abbreviations: CB = cerebellum; Hipp = hippocampus; Ctx = cortex; Coll = superior and inferior colliculus. Neither drug significantly reduced [^{125}I]iodo-ASEM accumulation in any of these regions ($P > 0.05$, ANOVA). The study demonstrates that [^{125}I]iodo-ASEM is α7-nAChR selective *in vivo* versus the 5-HT$_3$receptor and the main cerebral α4β2 -nAChR subtype.

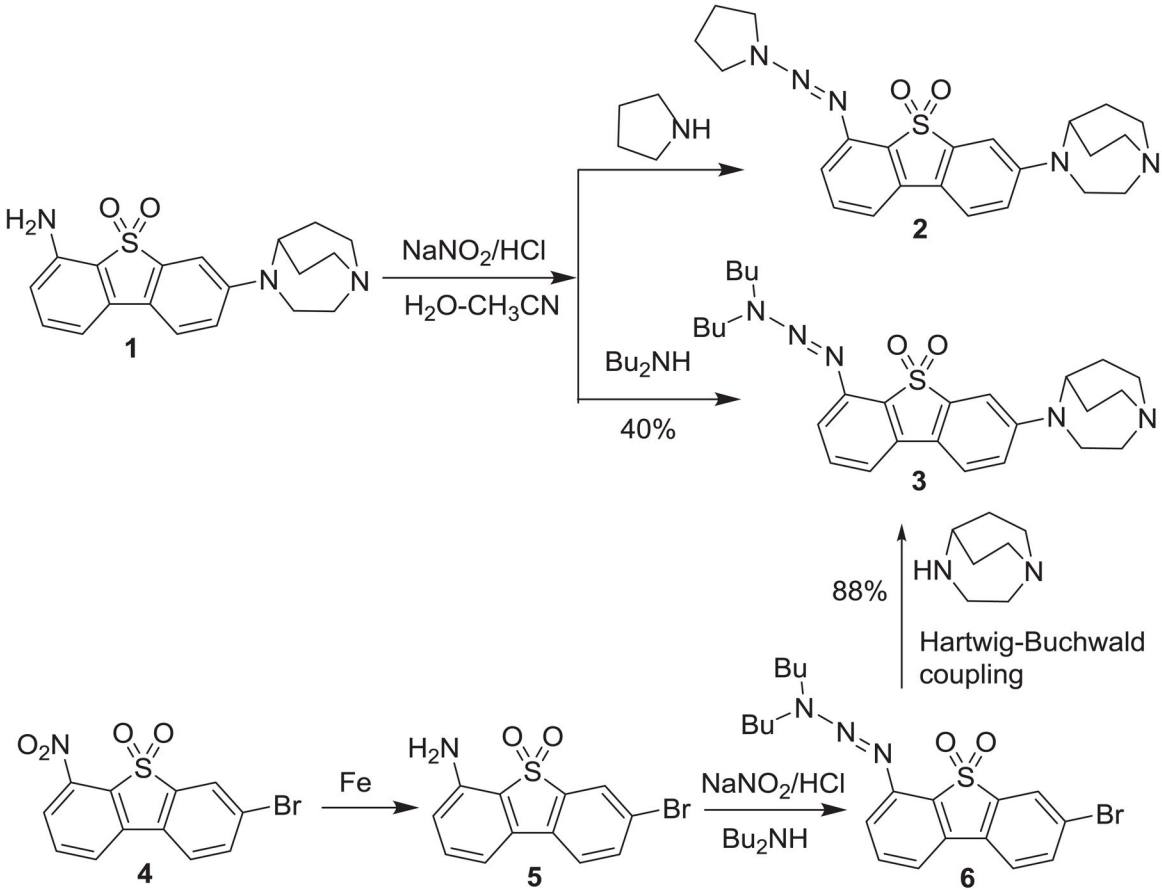

Scheme 1.

Synthesis of precursors **2** and **3** for radiosynthesis of [^{125}I]iodo-ASEM.

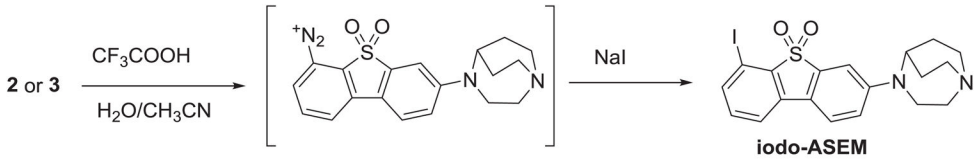

Scheme 2.
Model iodination of **2** and **3.**

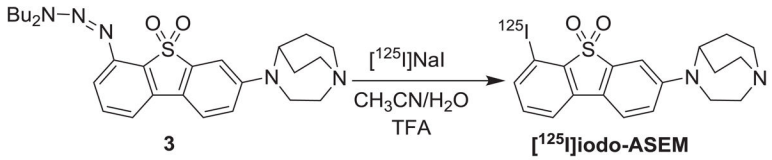

Scheme 3.
Radiosynthesis of [^{125}I]iodo-ASEM

Table 1

Binding affinity of iodo-ASEM. values are mean ± SEM (n=3)

nAChR subtype	K_i, nM	α7-nAChR Binding selectivity
α7 (rat)	0.5 ± 0.2	
α3β4 (human)	45 ± 8	α7/α3β4 = 90
α4β2 (human)	1707 ± 373	α7/α4β2 = 3,414

Table 2

Regional brain distribution of [^{125}I]iodo-ASEM in CD-1 mice. Data: mean %ID/g tissue ± SD (n=3)

Region	5 min	20 min	60 min	120 min	180 min	240 min	360 min
Cerebellum	4.25±0.42	5.20±2.08	2.56±0.35	1.41±0.08	0.76±0.15	0.38±0.05	0.21±0.04
Hippocampus	3.63±0.40	5.09±0.86	4.40±0.12	3.40±2.03	2.66±0.58	1.70±0.28	0.97±0.12
Cortex	4.78±0.47	6.25±0.28	6.50±0.57	4.29±0.42	2.74±0.55	1.40±0.06	0.72±0.12
Superior & inferior Colliculi	4.09±0.71	5.50±0.51	5.14±0.20	4.37±0.57	3.16±0.75	1.50±0.28	0.87±0.08
Rest of brain	3.89±0.42	4.90±0.24	4.60±0.18	3.24±0.26	2.09±0.40	1.051±0.10	0.57±0.05